Chapter 4

2D-3D Hybrid Model Using Overlapping Method

4.1 Introduction

In order to make timely prediction for issuing tsunami warnings and to clarify the fluid force acting on the structures around coastal area, the purpose of this study is to develop a 2D-3D hybrid tsunami model using the overlapping method based on the stabilized finite element method. This model simulates the tsunami wave propagation from the wave source area to the offshore area by 2D analysis that aiming for reducing the computational burden, and the area around the structures is simulated by 3D analysis that aiming for computing the fluid force precisely.

In this chapter, the overlapping method based on arbitrary domain coupling 2D and 3D analysis model by satisfying the conservation and compatibility conditions between 2D and 3D is introduced. Several numerical examples are performed to investigate the validity and efficiency of the hybrid model.

4.2 2D-3D Overlapping Method

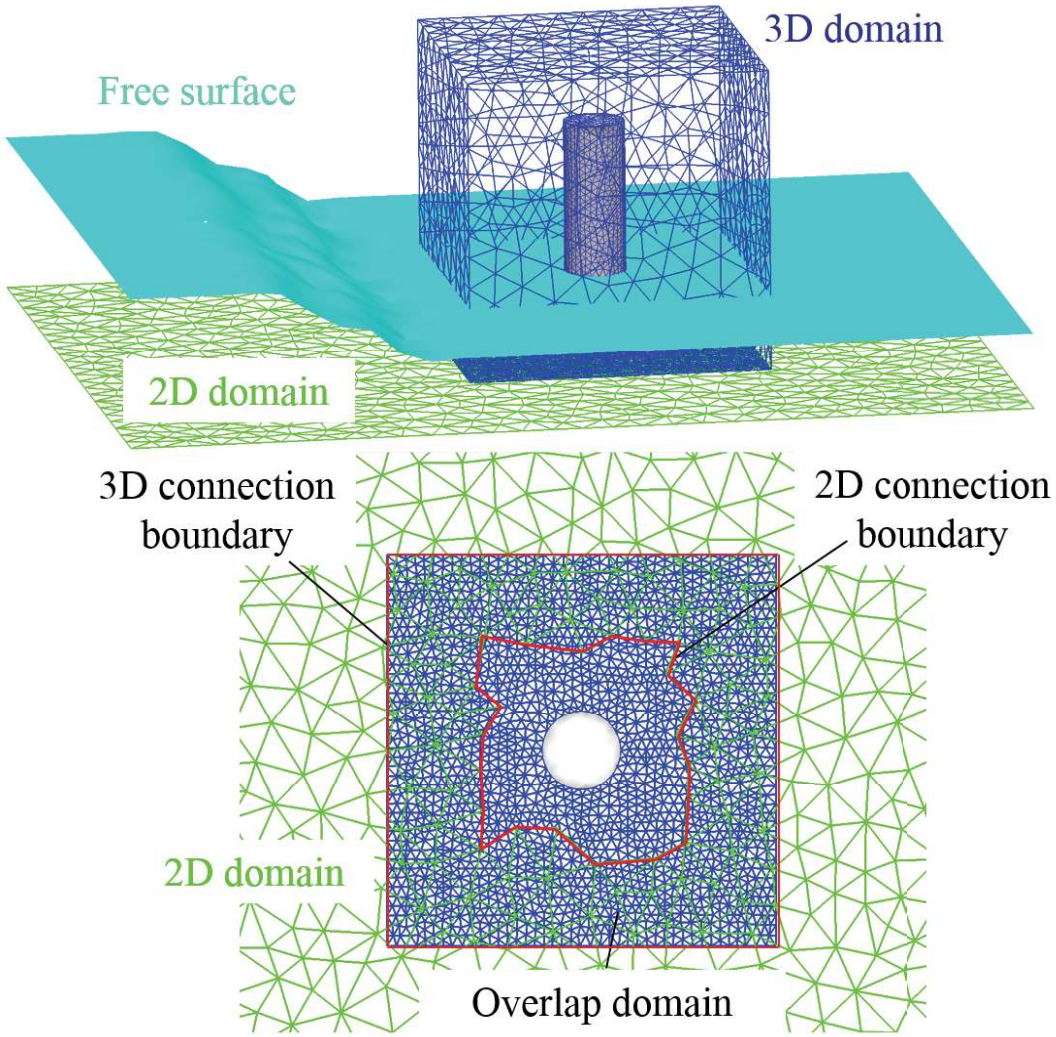

Figure 4.1 **Overlapping method**

In the previous study, the 2D-3D overlapping method [80] based on structured grid have been presented. For the overlap domain, the border is shared by the 2D domain and 3D domain, so that special treatment should be taken to generate the meshes for complex geometry. This results in the limited application. In this study, we develop the 2D-3D overlapping method into arbitrary grid, the definition is shown in **Figure 4.1**. In this method, the computational domain is separated into a 2D domain and a 3D domain. A overlap domain for the 2D and 3D domains is set. The domains and

the meshes of 2D and 3D can be arbitrary. Then the inner boundary of the 2D domain is defined as a 2D connection boundary, while the outer boundary of the 3D domain is defined as a 3D connection boundary. At the 2D connection boundary and the 3D connection boundary, the nodes of 2D and 3D can be located at different places. For the computation, the flow velocities and the water depth computed from the 3D domain are used as the boundary conditions of the 2D connection boundary. As the same, the flow velocities and the water depth computed from 2D domain are used as the boundary conditions of the 3D connection boundary. For the computation of real terrain tsunami simulation, the 3D domain can be chosen anywhere we want to compute precisely. Because of the place for the nodes of 2D and 3D is different, the boundary condition of 2D/3D connection boundary should be computed by making interpolation.

The details of the computation for the boundaries are presented in the following sections.

4.3 The Flowchart of the 2D-3D Overlapping Method

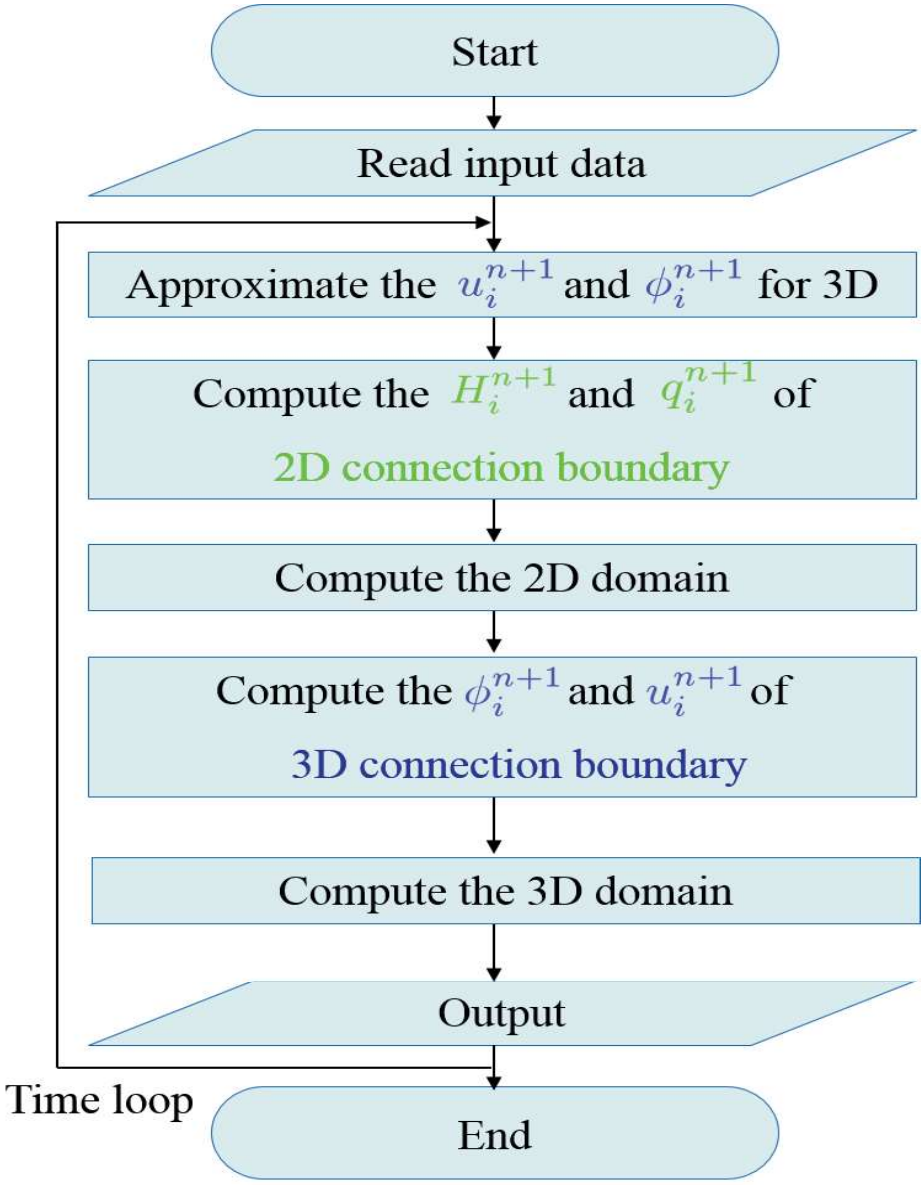

Figure 4.2 **Flowchart for 2D-3D overlapping method**

The flowchart of the 2D-3D overlapping method is shown in **Figure 4.2**.

Firstly, to approximate the flow velocity u_i^{n+1} and the phase function ϕ_i^{n+1} of n+1

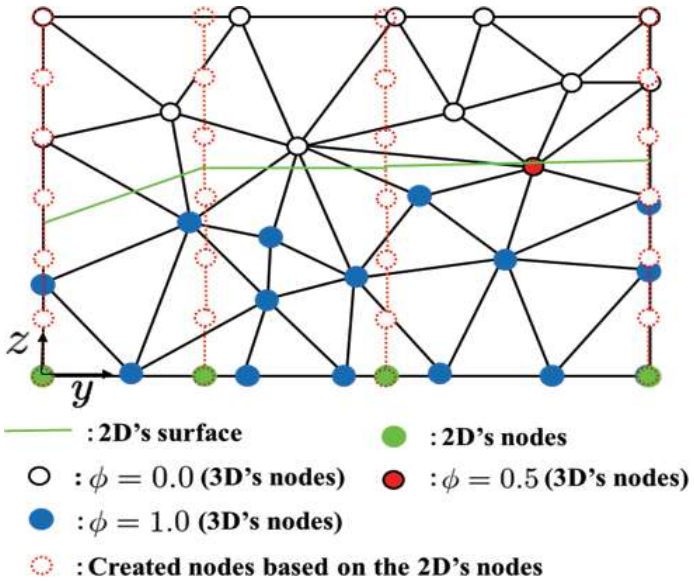

Figure 4.3 **Cross sectional view at the 2D connection boundary**

step for the 3D domain using the following equations.

$$u_i^* = \frac{3}{2}u_i^n - \frac{1}{2}u_i^{n-1}, \tag{4.1}$$

$$\phi_i^* = \frac{3}{2}\phi_i^n - \frac{1}{2}\phi_i^{n-1}, \tag{4.2}$$

$$u_i^{n+1} \approx 2u_i^* - u_i^n, \tag{4.3}$$

$$\phi_i^{n+1} \approx 2\phi_i^* - \phi_i^n, \tag{4.4}$$

where u_i^*, ϕ_i^* are approximated by the second order accuracy Adams-Bashforth method.

Secondly, to compute the boundary conditions of the 2D connection boundary by using u_i^* and ϕ_i^*. **Figure 4.3** is a cross sectional view of the 2D connection boundary. In this figure, auxiliary nodes S_i are set above the nodes of 2D boundary in the same distance. Then to find the auxiliary nodes belong to which elements. The values of the phase function $\phi_{s_i}^{n+1}$ and the flow velocity $u_{i_{s_i}}^{n+1}$ of the auxiliary nodes are computed out by making interpolation in the tetrahedron elements using

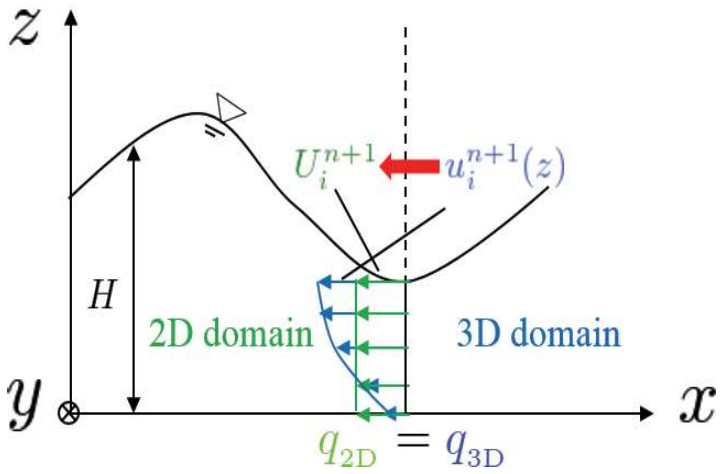

Figure 4.4 **Flow rate preservation condition at the 2D connection boundary**

the following interpolation equations,

$$\phi_{s_i}^{n+1}(x,y,z) \approx \sum_{\alpha=1}^{4} N_\alpha^e(x,y,z)\phi_\alpha^{n+1}, \tag{4.5}$$

$$u_{i_{s_i}}^{n+1}(x,y,z) \approx \sum_{\alpha=1}^{4} N_\alpha^e(x,y,z)\phi_\alpha^{n+1}. \tag{4.6}$$

Then to substitute the values of the auxiliary nodes into the following integral equations, the boundary conditions of the 2D connection boundary can be obtained (see **Figure 4.4**).

$$H_i^{n+1} = \int \phi_{s_i}^{n+1}(z)dz, \tag{4.7}$$

$$q_i^{n+1} = U_i^{n+1}H_i^{n+1} = \int \phi_{s_i}^{n+1}(z)u_{i_{s_i}}^{n+1}(z)dz. \tag{4.8}$$

Then to compute the 2D domain by using the the boundary conditions of the 2D connection boundary.

Thirdly, to compute the boundary conditions of the 3D connection boundary. **Figure 4.5** shows how to compute the phase function at the 3D connection boundary. We compare the water depth H_{2D} with those of the nodes at the 3D connection boundary, then they can be separated into four cases in **Figure 4.5**. In the figure, $Z_{P_{3D}}$ is the coordinate value in the vertical direction of node P_{3D}. d is the distance from node P_{3D} to the wave surface of 2D. h_e is the representative length of the

tetrahedron element. About the flow velocity for the 3D connection boundary, the average flow velocity computed by 2D is used (see **Figure 4.6**).

$$u_i^{n+1} = U_i^{n+1}, i = 1, 2, \tag{4.9}$$

$$u_3^{n+1} = 0. \tag{4.10}$$

Finally, to compute the 3D domain by using the boundary conditions of the 3D connection boundary and the 3D numerical model, to output the results and to do the time loop.

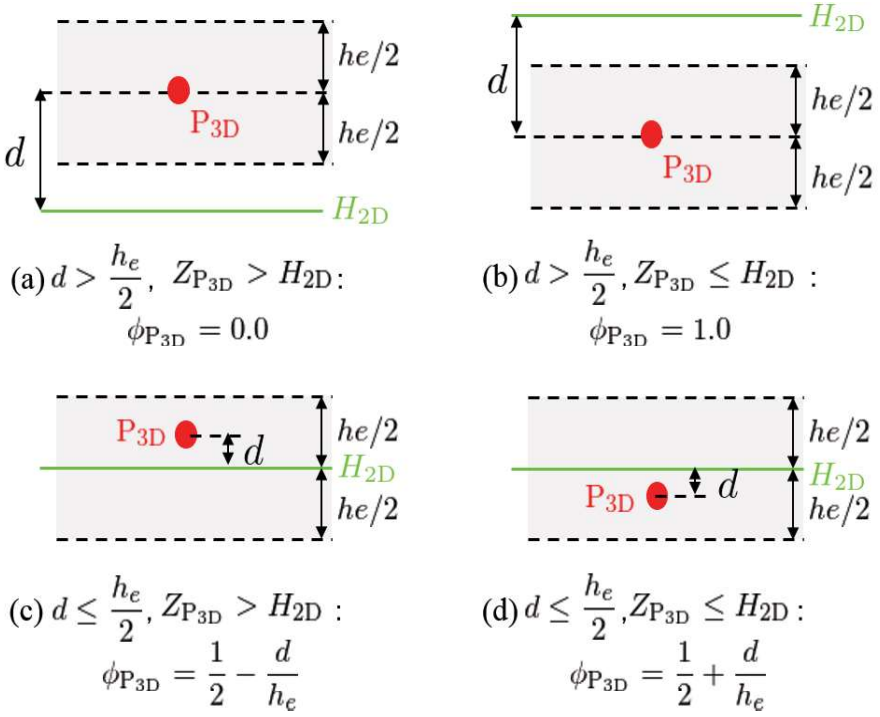

Figure 4.5 **Computation of the phase function at the 3D connection boundary**

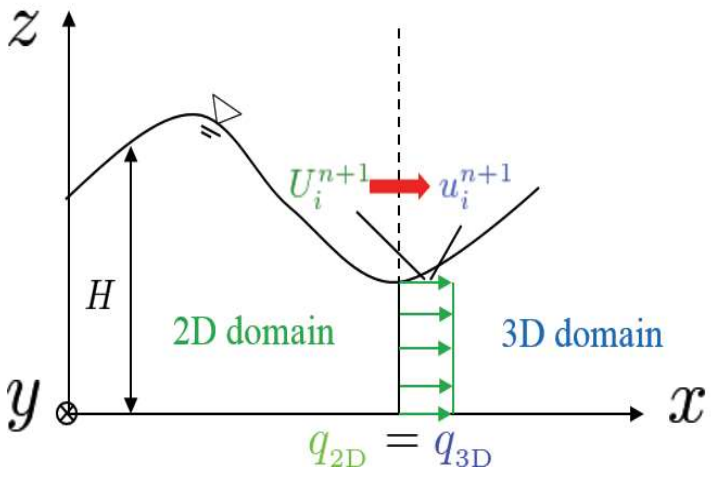

Figure 4.6 **Flow rate preservation condition at the 3D connection boundary**

4.4 Switch Model for Improving Efficiency

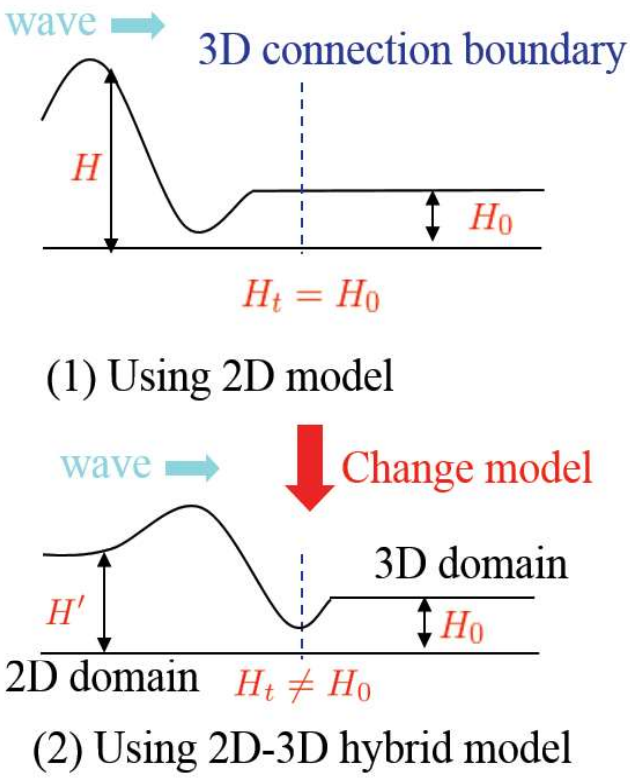

Figure 4.7 **Switch Model**

For the large-scale simulation, it may take a lot of computational time for wave propagation from source area to an target 3D area, such as a real terrain tsunami simulation. In order to increase the efficiency by reducing computational memory and computational time, a switch model is presented in this section. **Figure 4.7** shows the conceptual diagram of the switch model. In this model, the water depth H_t is checked at the 3D connection boundary by every step, before the wave coming to the 3D connection boundary ($H_t = H_0$), all the target computational area is computed by the 2D model. When the wave reach the 3D connection boundary ($H_t \neq H_0$), the target computational area is separated into 2D and 3D domain and computed by the 2D-3D hybrid model. Then the flowchart is changed into **Figure 4.8**. However, for the small computational area, we can just adopt the flowchart shown in **Figure 4.2**.

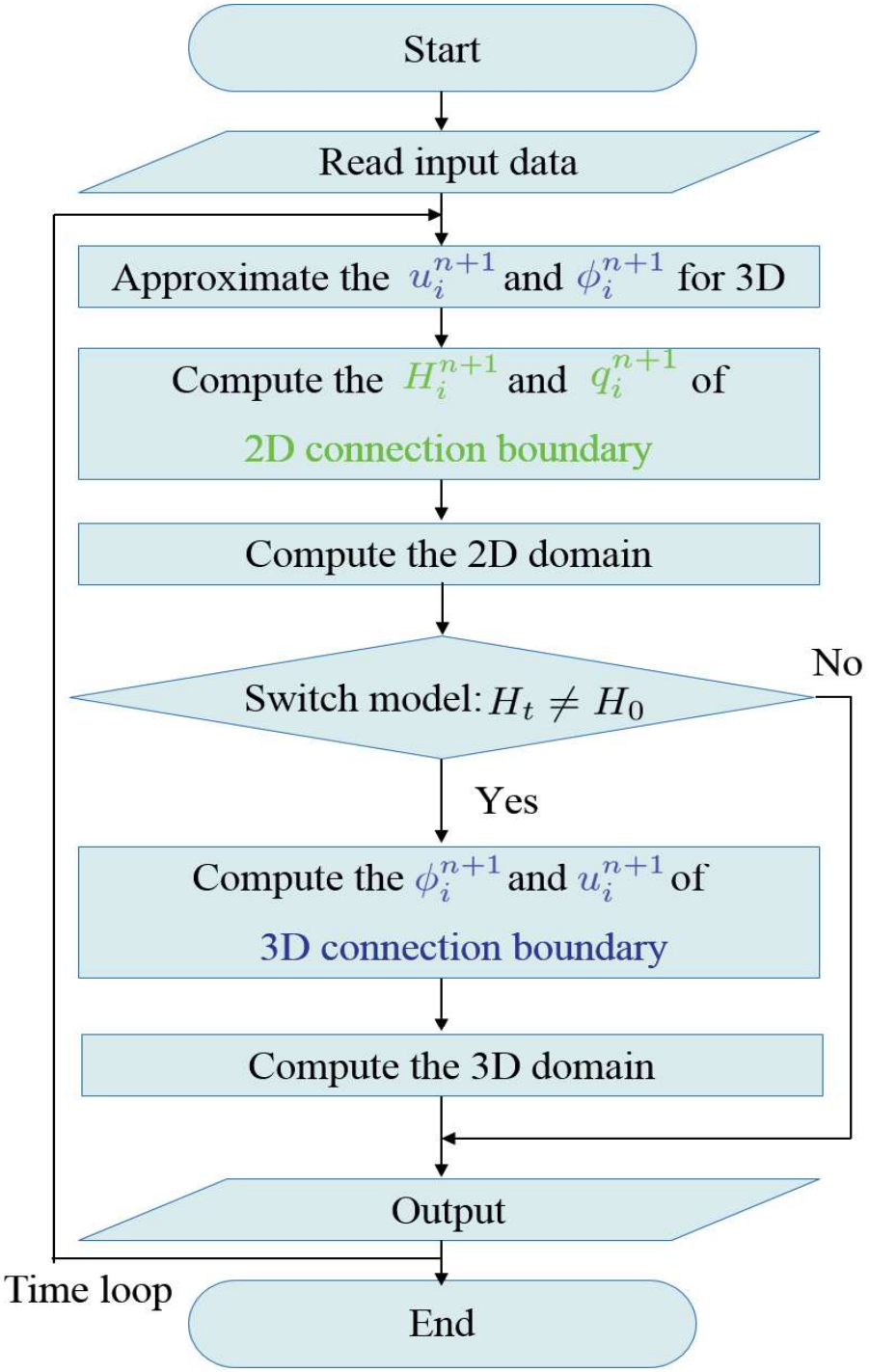

Figure 4.8 **Flowchart of the 2D-3D overlapping method with a switch model**

4.5 Numerical Examples

4.5.1 Dambreak with Structures

Figure 4.9 shows two computational models to test the performance of the 2D-3D hybrid model. In order to increase the efficiency of the 2D-3D hybrid model, both of the computational models are computed by the 2D at first before the wave propagating to the 3D domain. Then when the wave reaches the 3D domain, the hybrid model begins to work. For the Case B, the 3D domain rotates 45° from Case A to show the possibility that the wave can propagate from different directions. For the computational conditions, the mesh size of the 2D domain is 0.1m and the mesh size of the 3D domain is 0.05m, The coupling domain is set to be 0.4m (see to **Figure 4.10**). The time increment is 0.001s and the boundary condition is slip condition.

Several snapshots of surface profiles are shown in **Figure 4.11**. From these figures, we can see from $t = 0.80$s to $t = 2.25$s, the 2D analysis model changes into 2D-3D hybrid model when the wave reaches the 3D domain. We can also confirm that the 2D-3D hybrid model solve this computational problem stably. **Figure 4.12** shows the time history of water depth variation at P(12.5, 0.0), we can see both the results are almost the same. The arbitrary choices of the 3D domain and the grids have been shown.

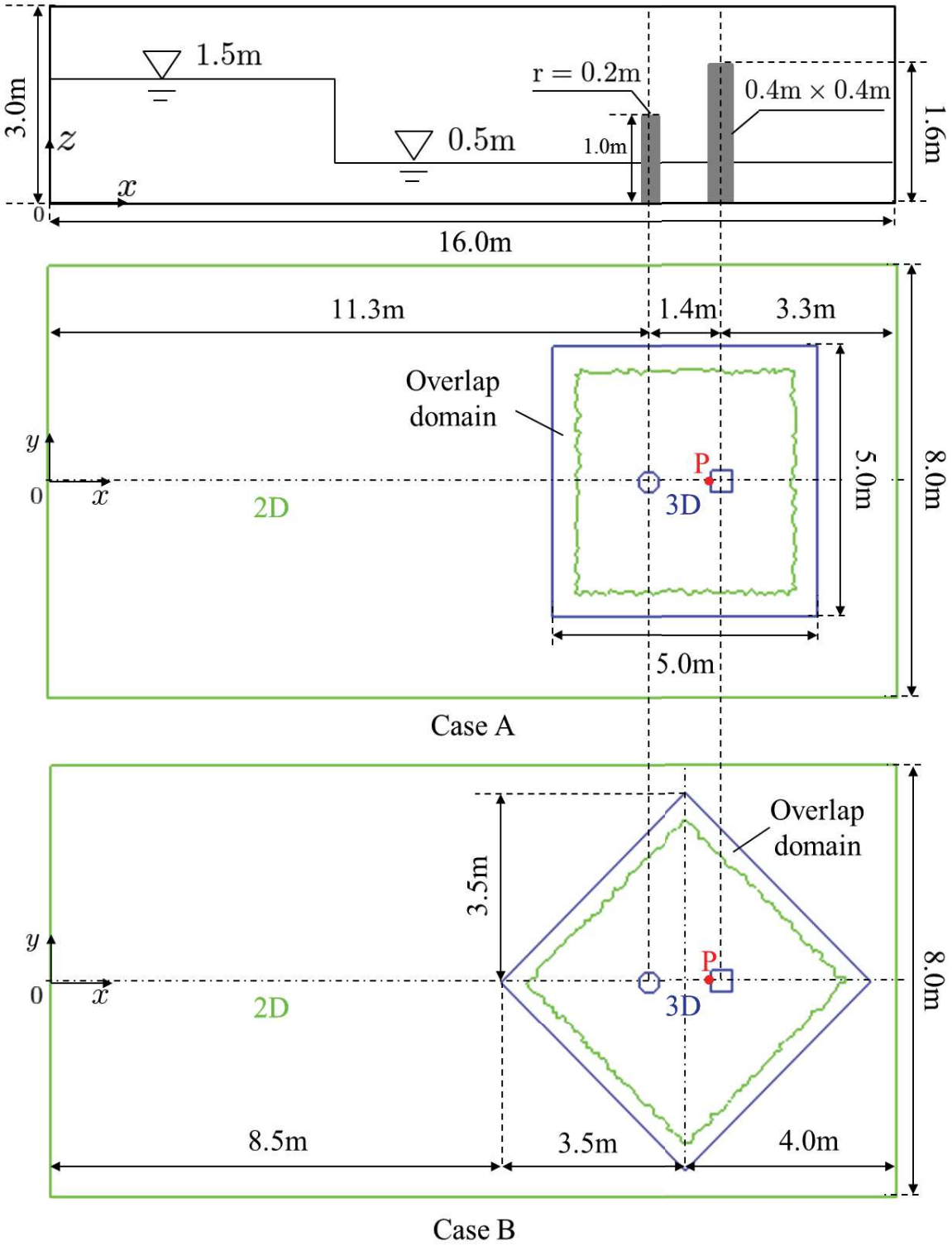

Figure 4.9 **Computational models**

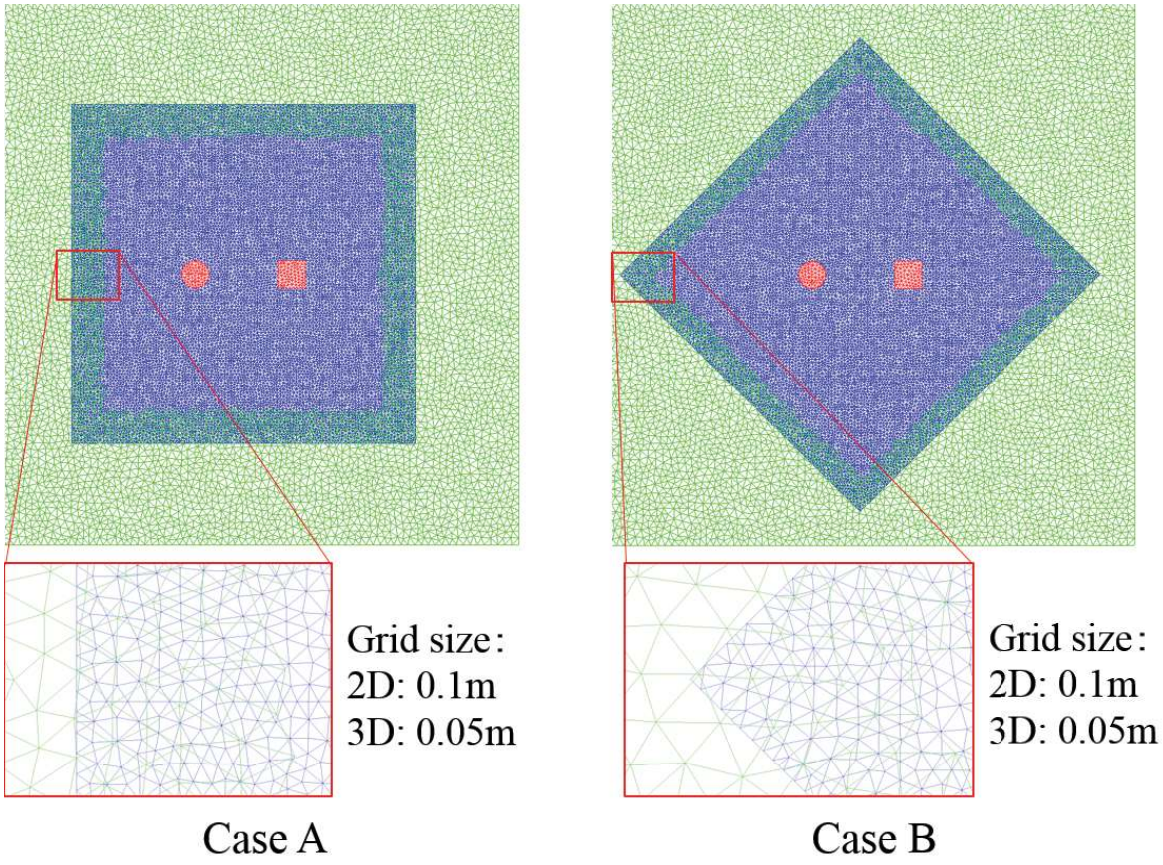

Figure 4.10 **Computational mesh**

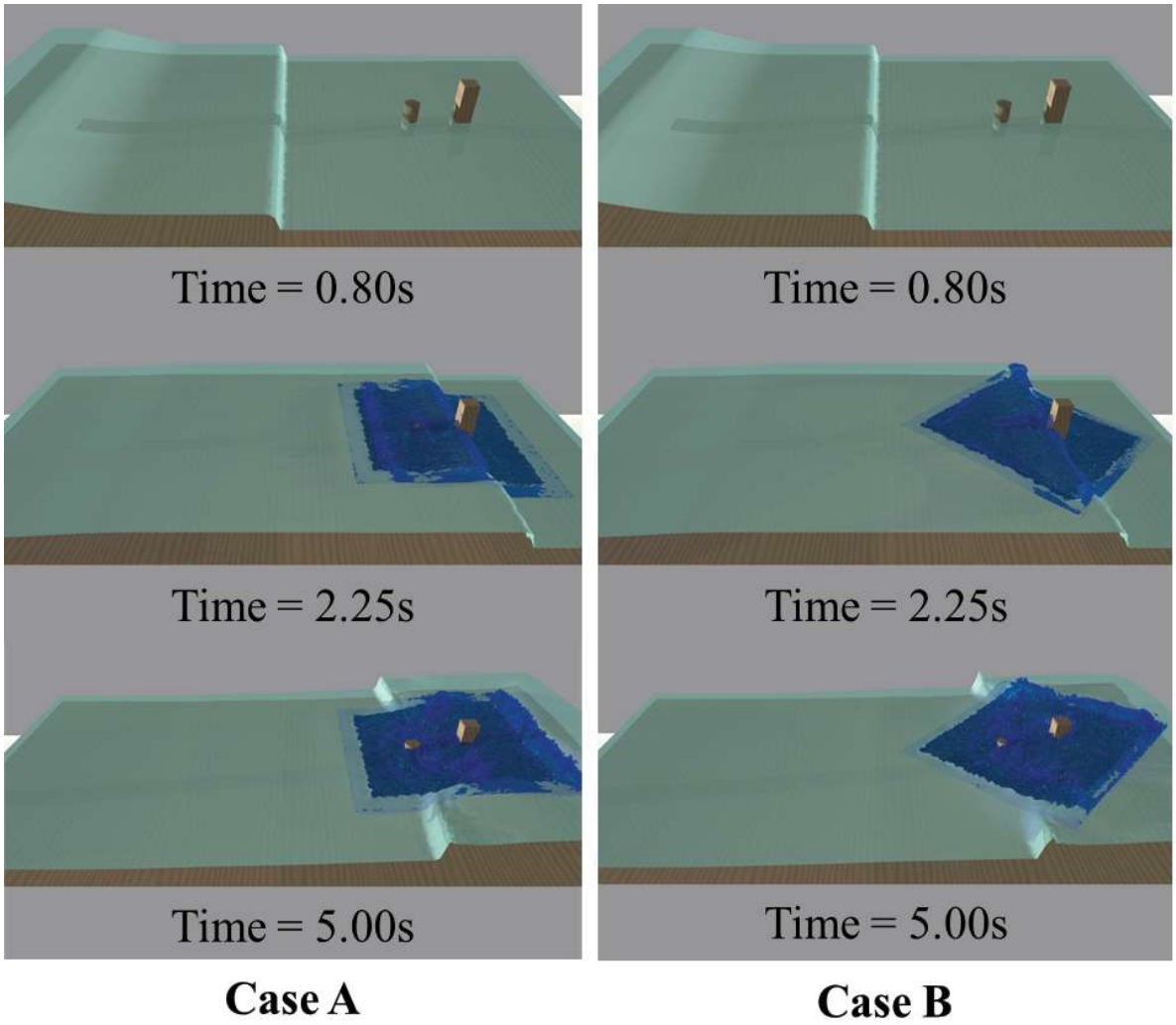

Figure 4.11 **Snapshots of surface profiles**

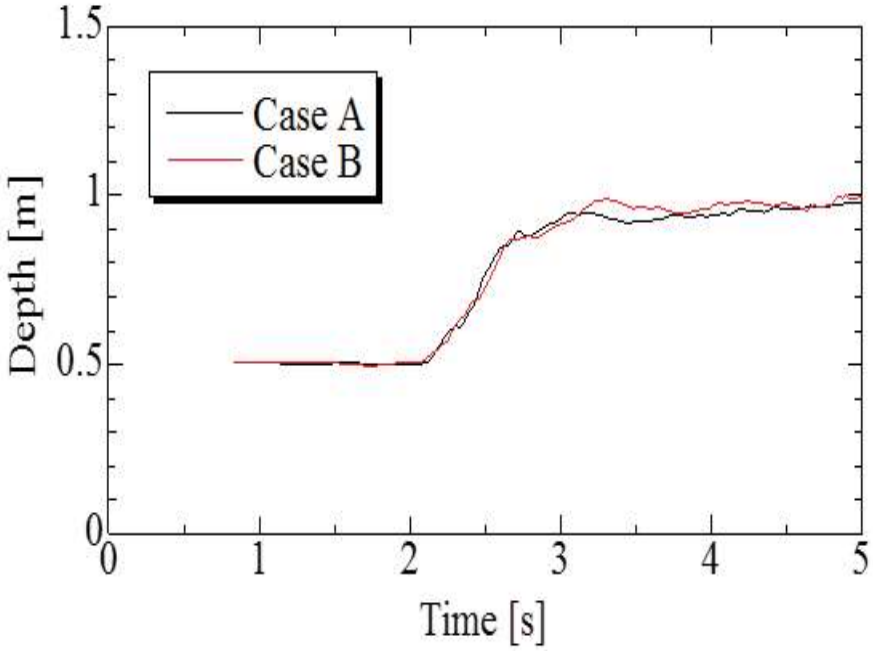

Figure 4.12 **Time history of water depth variation at P(12.5, 0.0)**

4.5.2 Runup of Solitary Wave Problem

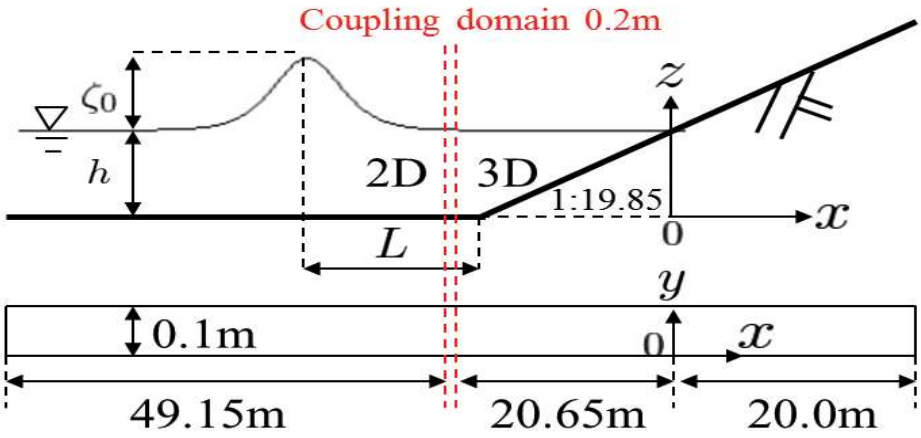

Figure 4.13 **Computational model**

The runup of a solitary wave problem shown in **Figure 4.13** is simulated to investigate the applicability of the 2D-3D hybrid model (using the VOF method) for structure mesh and unstructured mesh. Besides, the comparison between using the VOF method and the PFM is made. The results are compared to the experimental results [81], results of the 2D and 3D analysis models. For the initial conditions, the initial wave height is set by the following equation,

$$\zeta(x, t = 0) = \frac{\zeta_0}{h}\text{sech}^2\sqrt{\frac{3\zeta_0}{4h}}(x - x_0), \tag{4.11}$$

the ratio of the wave height ζ_0 and depth h is set to be 0.3. x_0 is the location of wave crest. The initial flow velocity is set by the following equation,

$$u(x, t = 0) = \zeta(x, t = 0)\sqrt{\frac{g}{h}}. \tag{4.12}$$

The wave crest is located at the half solitary wave length from the front end of the slope.

$$L = \sqrt{\frac{4h}{3\zeta_0}}\text{arccosh}\Big(\sqrt{\frac{1}{0.05}}\Big). \tag{4.13}$$

Figure 4.14 shows the meshes around the connection boundary, the mesh size is set to be 0.05m, the width of the overlap domain is set to be 0.2m (4 elements) in this

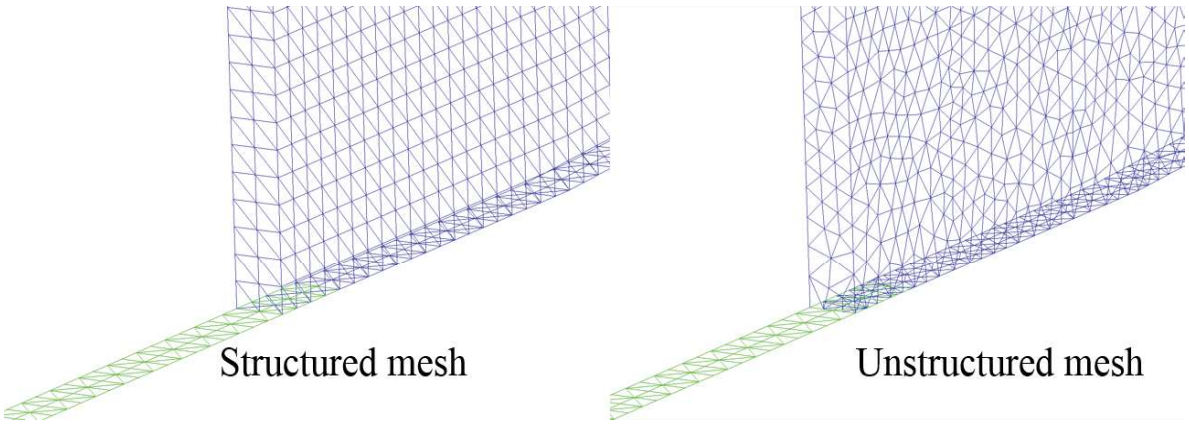

Figure 4.14 **Mesh around the connection boundary**

case. Structured mesh and unstructured mesh are used in 3D domain for comparison. The slip boundary condition is applied for the wall and the bottom. The kinematic viscosity coefficient ν_e is set to be $1.0 \times 10^{-3}\mathrm{m}^2/\mathrm{s}$, the Manning coefficient n is set to be $0.01\mathrm{s}/\mathrm{m}^{\frac{1}{3}}$ for the 2D analysis.

The comparisons of the surface profiles at different non-dimensionalized times ($t' = t\sqrt{\frac{g}{h}} = 10, 15, 20, 30$) are shown in the **Figure 4.15**. In the figure, Exp. denotes the experimental result, S.W.E. denotes the result by solving the 2D shallow water equations, N.S.E. denotes the result by solving the 3D Navier-Stokes equations, S.W.E.+N.E. denotes the result by using the 2D-3D hybrid model. From the figure, we can see the results of 3D is the best agree with the experimental results. The results of the 2D-3D hybrid model show better agree with the experimental results than the results of 2D. And the difference can be ignored between using the structured mesh and the unstructured mesh for the 2D-3D hybrid model.

From the **Figure 4.16**, the peak value of the result by using the PFM is better agree to the experimental result than using the VOF method at $t' = 20$. **Figure 4.17** shows the free surface near the overlap domain at $t = 4.0\mathrm{s}$. From the figure, we can see the surface is more smoothly connected by using the PFM.

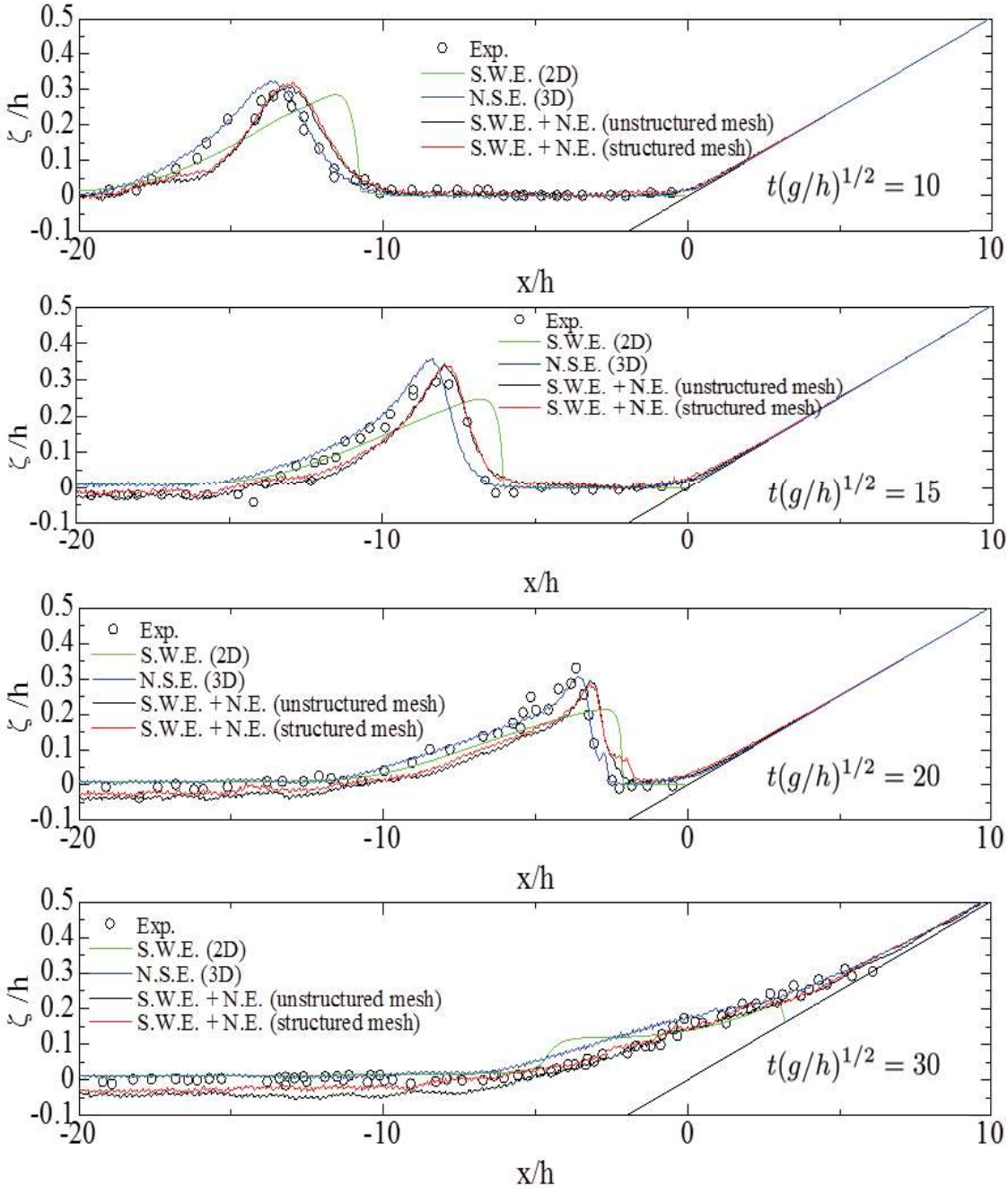

Figure 4.15 **Comparison of surface profiles**

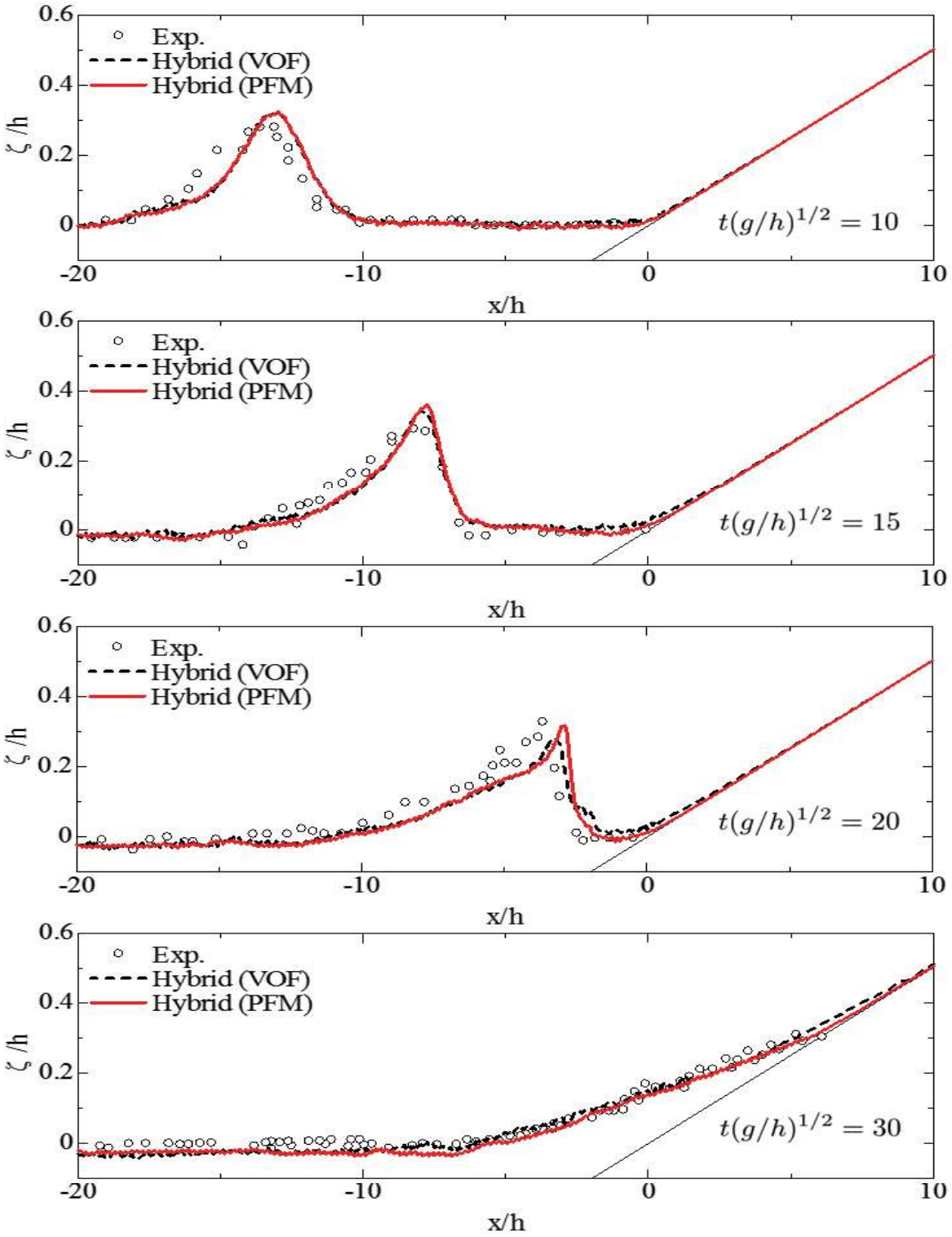

Figure 4.16 **Comparison of the surface profiles**

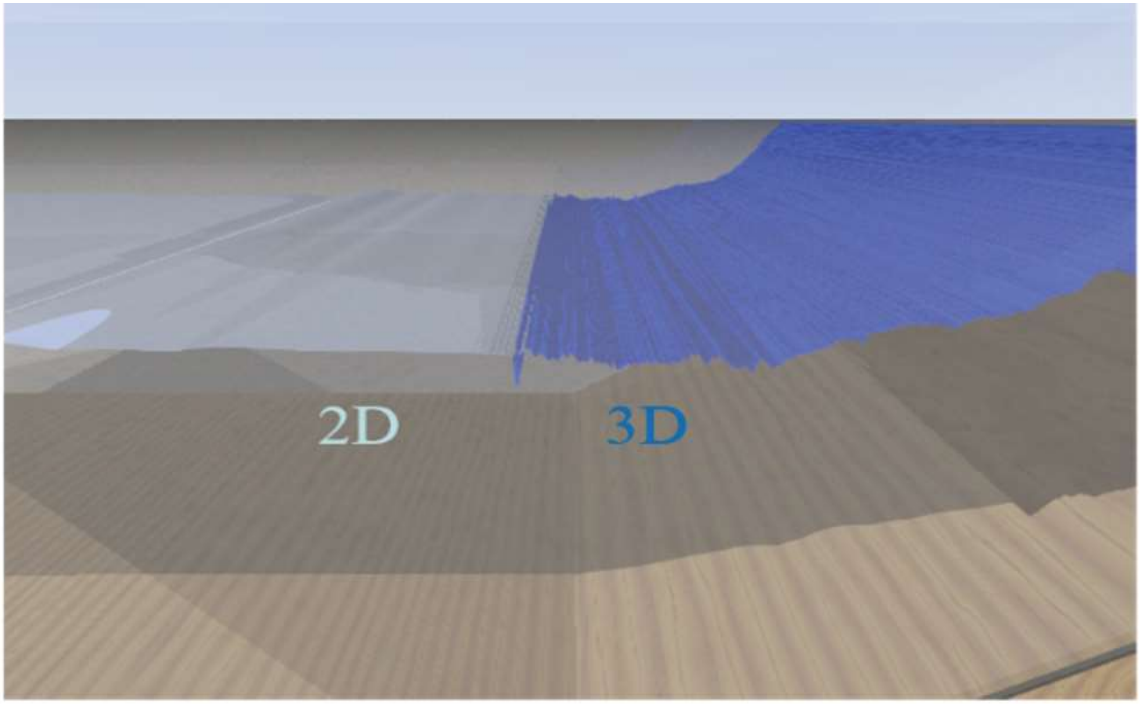

(A) 2D-3D Hybrid Model using VOF method

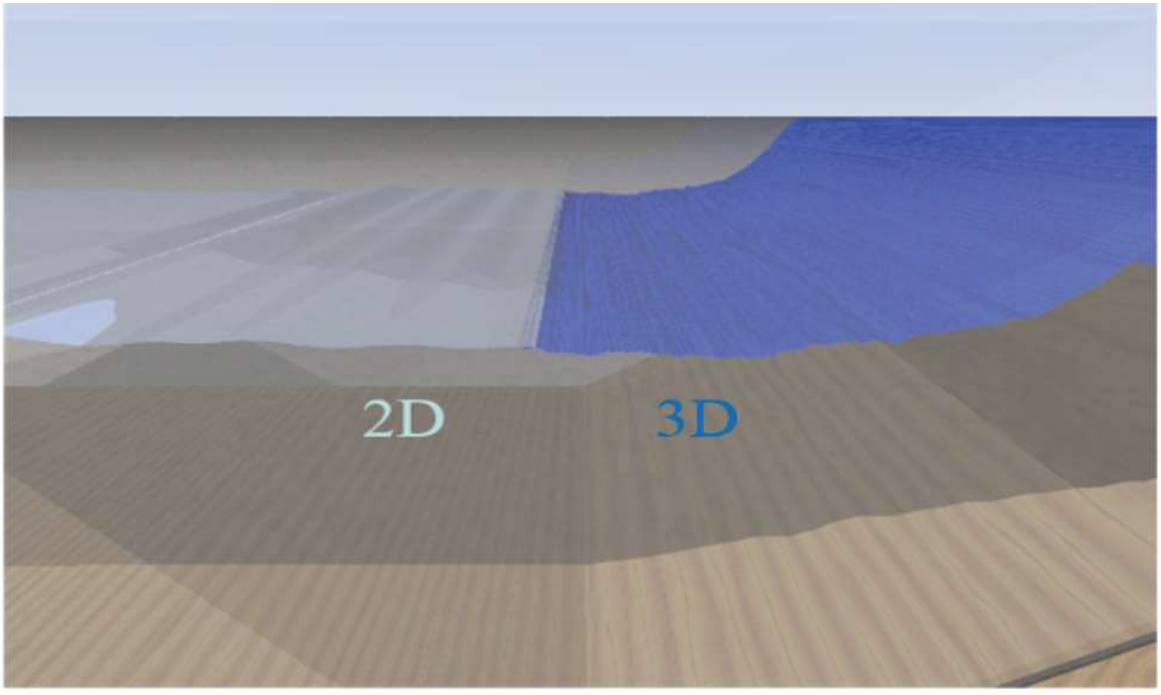

(B) 2D-3D Hybrid Model using PFM method

Figure 4.17 **Free surfaces near the overlap domain at** $t = 4.0$**s**

4.5.3 Wave Problem Around a Breakwater

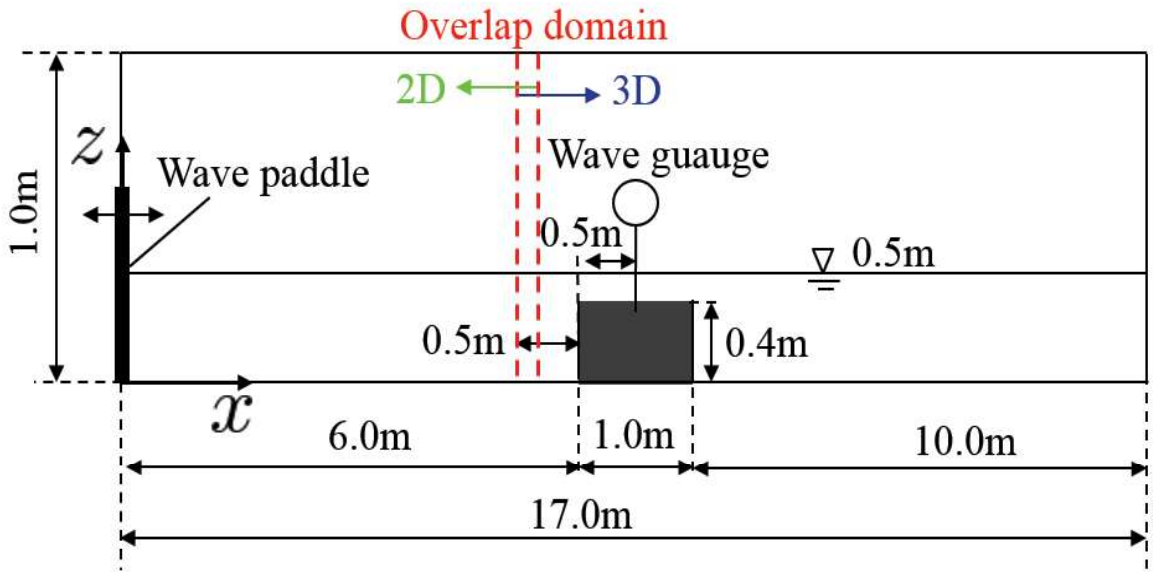

Figure 4.18 **Computational model**

In order to investigate the influence of the width of the overlap domain for the 2D-3D hybrid model, the wave problem around a breakwater (**Figure 4.18**) is simulated. In this problem, a wave maker is set on the left side of the model. Two cases of Cnoid wave are applied. For the case A, the wave height is 0.05m, the period is 2.0s. For the case B, the wave height is 0.075m, the period is 1.0s. The mesh size of 2D domain is 0.01m. About the 3D domain, the mesh around the breakwater is 0.01m and the other place is 0.02m (see **Figure 4.19**). The slip boundary condition is applied for the wall of the aquarium, and the time increment is 0.001s.

Figure 4.20 and **Figure 4.21** show the time history of water level variation of the wave gauge for the two cases. In the figures, the circle line denotes the experimental results [72], each solid line shows the result by changing the width of the overlap domain. For the case A, we can see all the analysis results are in good agree with the experimental results. For the case B, we can see the results of the overlap domain that more than 0.04m (4 elements) are in better agree with the experimental results than the results of 0.01m (1 element) and 0.02m (2 elements). In conclusion, for the width of the overlap domain, it is better to set more than 4 elements, but considering

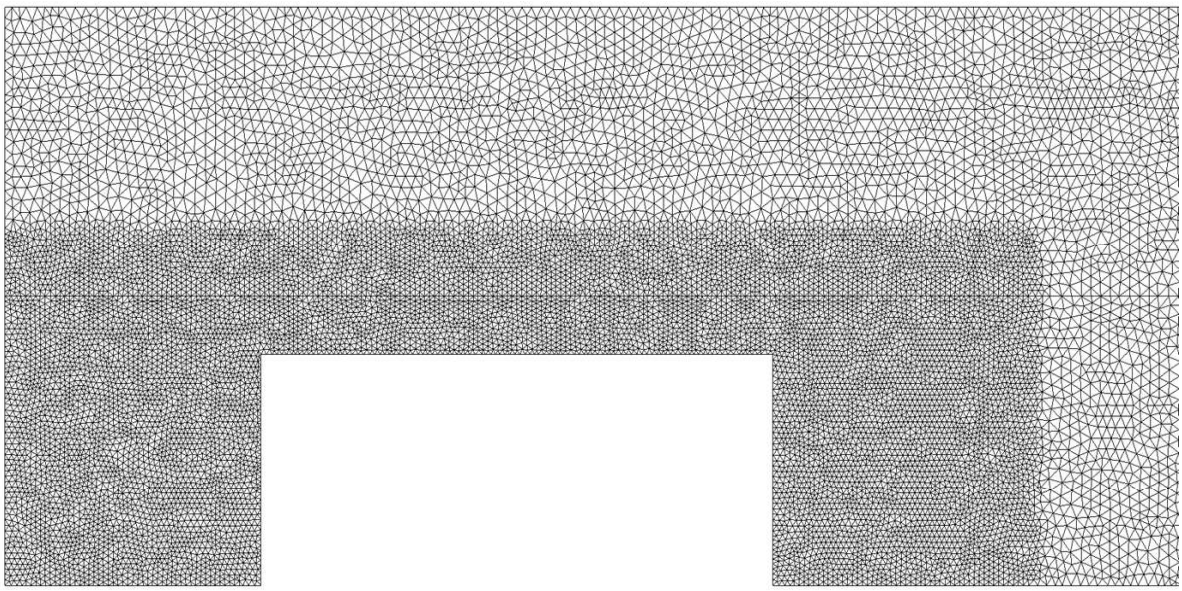

Figure 4.19 **Mesh around the breakwater**

about the computational cost, 4 elements can be good.

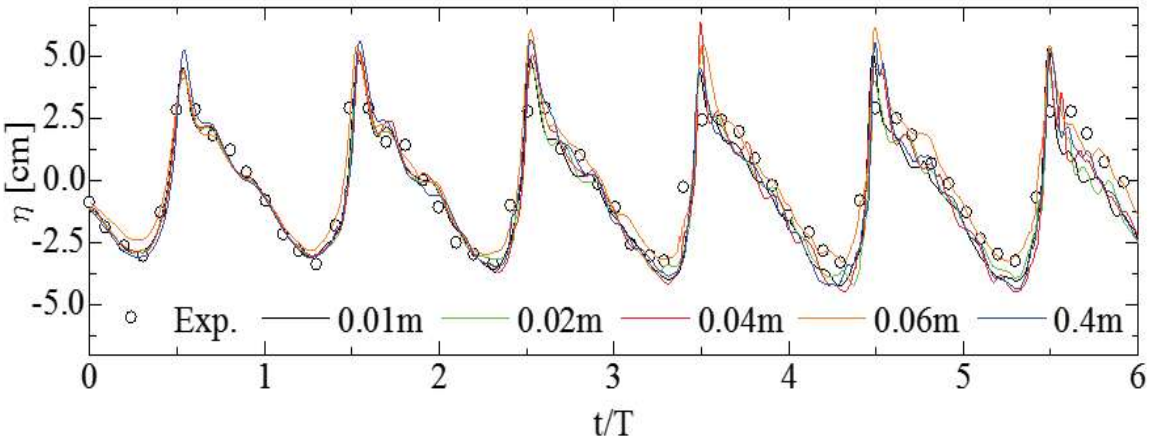

Figure 4.20 **Time history of water level variation for case A**

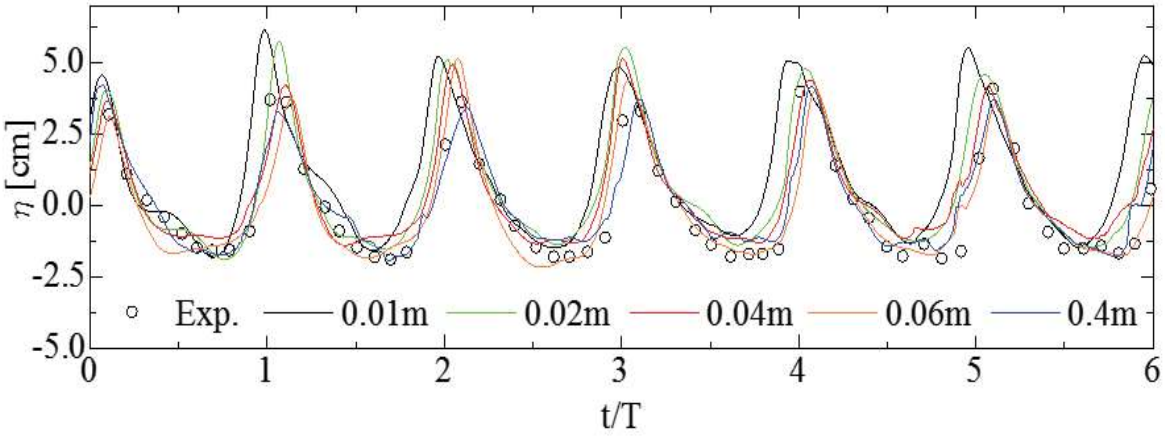

Figure 4.21 **Time history of water level variation case B**

4.6 Chapter Summary

In this chapter, the 2D-3D hybrid tsunami model using the overlapping method based on an arbitrary mesh is developed. Several numerical examples have been tested, and the following remarks can be concluded:

- From example of the dambreak with structures, the options for choosing the 3D domain have been shown. And the computation is stable for the wave propagating from bidirection of 2D domain and 3D domain.
- From the runup of solitary wave problem, the results of the 2D-3D hybrid model show better agree with the experimental results than the results of 2D. The 2D-3D hybrid model is suitable for using structured mesh and unstructured mesh. And the 2D-3D hybrid model using the PFM shows better results than the one using the VOF method.
- From the wave problem around a breakwater, to choose the width of overlap domain for about 4 elements can give a reasonable result.

From the above remarks, the effectiveness of the present 2D-3D hybrid model has been confirmed.